Supporting Information. Comparing approaches for estimating ecological connectivity at a local scale in a marine system.

SECTION 1

Table S1: Substrate class suitability for kelp habitat. Substrate types are from Greenlaw et al. (2013).

Substrate class	Suitable habitat for kelp (1 = yes, 0 = no)
Boulders	1
Continuous bedrock	1
Discontinuous bedrock	1
Other	0
Mixed sediment	0
Sand & gravel	0
Gravel	0
Mud	0
Sand	0
Sand & mud	0

Table S2: Release locations for propagules.

Species	Longitude (dd)	Latitude (dd)	Depth (m)
Laminarian kelps, *Membranipora membranacea*	-62.963	44.664	26
	-62.904	44.666	30
	-62.908	44.639	14
	-62.744	44.708	23
	-62.782	44.653	13
	-62.631	44.747	20
	-62.532	44.774	18
	-62.426	44.800	16
	-62.257	44.864	10
	-62.279	44.892	2
	-62.142	44.880	26
	-62.174	44.920	2
	-62.045	44.927	10
Stronglyocentrotus droebachiensis	-61.989	44.868	49
	-61.977	44.845	57
	-61.964	44.816	68
	-61.954	44.797	92
	-62.453	44.729	41
	-62.461	44.738	60
	-62.431	44.704	71
	-62.405	44.674	84
	-62.647	44.703	43
	-62.613	44.669	52
	-62.586	44.643	77
	-62.562	44.620	88
	-62.222	44.826	45
	-62.213	44.813	60
	-62.187	44.771	79
	-62.182	44.763	90

Table S3: Acoustic Doppler Current Profiler deployment information.

Location	Longitude (dd)	Latitude (dd)	Depth (m)	Sampling frequency (h)	ADCP data date range (mm/dd/yyyy)	Species
Liscomb	-62.0709	44.8523	53	0.5	02/07/2019 – 09/29/2019	*M. membranacea, S. droebachiensis*
Ship Harbour	-62.7651	44.7025	32.2	2	12/7/2018 – 09/24/2019	Laminarian kelps

Table S4: Summary of runs for particle tracking simulations. Number below species refers to interval at which particle locations were extracted from the model (e.g. every 96 hours for *S. droebachiensis*).

Run number	Species	Release date	End simulation
1		2019-02-01 12:00	2019-04-02 12:00
2		2019-02-05 12:00	2019-04-06 12:00
3		2019-02-10 12:00	2019-04-11 12:00
4		2019-02-15 12:00	2019-04-16 12:00
5	*Stronglyocentrotus droebachiensis* (96 hours)	2019-02-20 12:00	2019-04-21 12:00
6		2019-03-01 12:00	2019-04-30 12:00
7		2019-03-05 12:00	2019-05-04 12:00
8		2019-03-10 12:00	2019-05-09 12:00
9		2019-03-15 12:00	2019-05-14 12:00
10		2019-03-20 12:00	2019-05-19 12:00
11		2019-07-01 12:00	2019-07-29 12:00
12		2019-07-05 12:00	2019-08-02 12:00
13		2019-07-10 12:00	2019-08-07 12:00
14		2019-07-15 12:00	2019-08-12 12:00
15	*Membranipora membranacea* (84 hours)	2019-07-20 12:00	2019-08-17 12:00
16		2019-08-01 12:00	2019-08-29 12:00
17		2019-08-05 12:00	2019-09-02 12:00
18		2019-08-10 12:00	2019-09-07 12:00
19		2019-08-15 12:00	2019-09-12 12:00
20		2019-08-20 12:00	2019-09-17 12:00
21		2019-10-15 12:00	2019-10-17 12:00
22		2019-10-20 12:00	2019-10-22 12:00
23		2019-10-25 12:00	2019-10-27 12:00
24		2019-10-30 12:00	2019-11-01 12:00
25	Laminarian kelps (12 hours)	2019-11-04 12:00	2019-11-06 12:00
26		2019-11-15 12:00	2019-11-17 12:00
27		2019-11-20 12:00	2019-11-22 12:00
28		2019-11-25 12:00	2019-11-27 12:00
29		2019-11-30 12:00	2019-12-02 12:00
30		2019-12-04 12:00	2019-12-06 12:00

Table S5: Accuracy results for random forest model used to predict the distribution of suitable habitat for kelp in the Eastern Shore Islands Area of Interest. Observational data were divided into training and validation sets by 2/3 and 1/3, respectively.

		Confusion matrix			
		Predicted			
Data usage		**Absent**	**Present**	**Class error (%)**	**Total error (%)**
Training (n = 330)	Absent	173	30	14.78	20.7
	Present	41	99	29.29	
Validation (n = 162)	Absent	84	22	20.75	21.7
	Present	14	46	23.3	

(Observed)

Table S6: Cost breakdown for applying the 3D approach including the development of a fine-scale regional physical ocean model and applying outputs to calculate dispersal trajectories for target species.

Model stage	**Item**	**Details of cost**	**Cost (CAD$)**
Development	Post-doctoral researcher	2-year model development	120 000
	Base model	Code and expertise from physical oceanographer	5 000
	Computation	256 CPUs utilized for 3 days week^{-1} for 15 months at \$7.155 per instance hour^{-1} (AWS pricing calculator 2023)	184 000
Validation	In-situ measurements	4 ADCPs, moorings, tide gauges, TS profiles	100 000
Operation	PhD student	2 months to run particle tracking simulations and process outputs	4 400
	Total		**413 400**

Table S7: Cost breakdown for applying the 2D approach to calculate dispersal area for a target species.

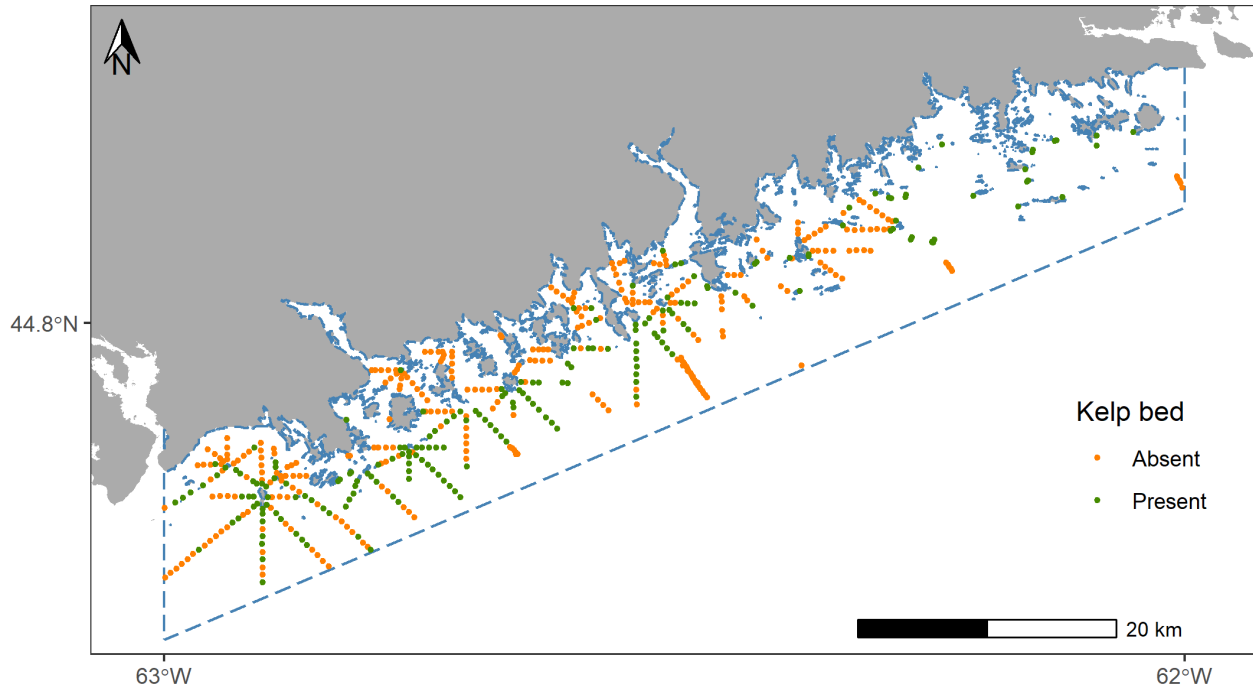| **Item**	**Details of cost**	**Cost (CAD)**
ADCP	Purchase price for instrument	20 000
Instrument deployment	Boat time and divers (2 days)	2000
Data analysis	Clean and process current data. Assemble input data for 2D approach and apply.	1 000
Total		**23 000**

Figure S1: Map of point location data used to train a random forest model to predict the distribution of suitable habitat for kelp within the Eastern Shore Islands (ESI) proposed Marine Protected Area (between 62° W and 63° W). The model domain is indicated by the blue outline and is bound by the 40-m isobath and longitudinal boundaries of the ESI.
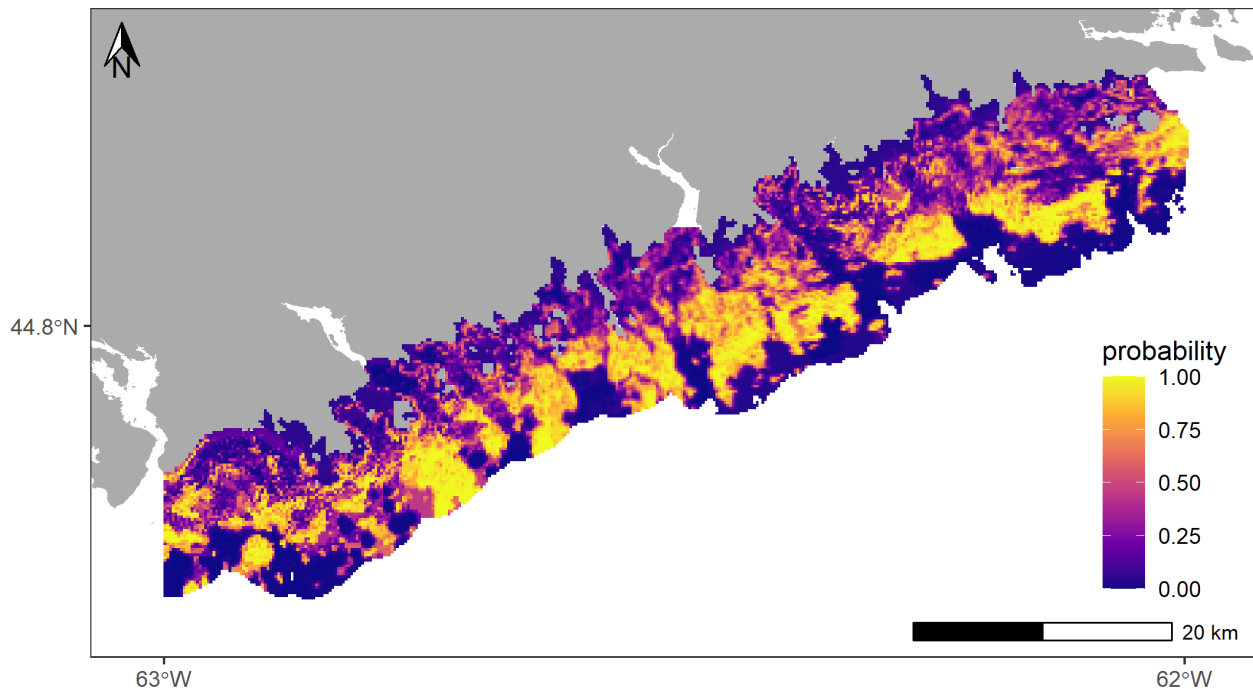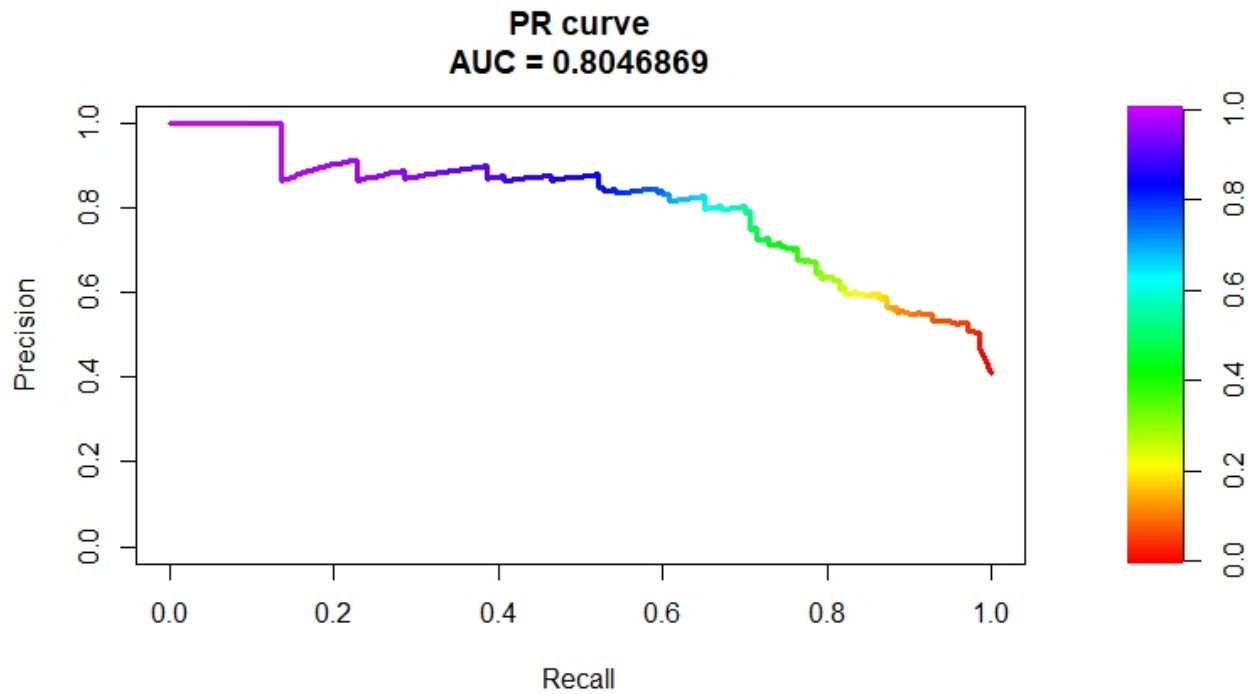

Figure S2: Map of raw probabilities from random forest model predicting the distribution of suitable habitat for kelp in the Eastern Shore Islands Area of Interest (between 62° W and 63° W).

PR curve
AUC = 0.8046869

Figure S3: Precision-recall curve for random forest model used to predict suitable habitat for kelp in the Eastern Shore Islands Area of Interest.
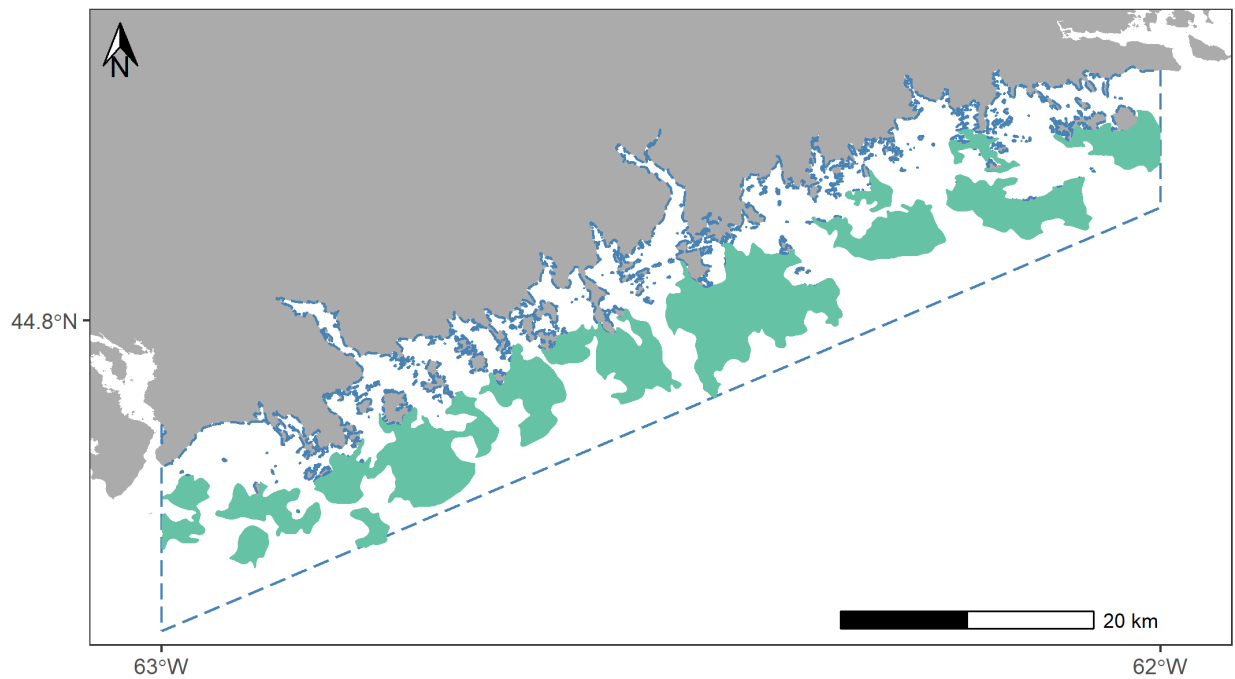
Figure S4: Map of kelp patches predicted from the random forest model within the Eastern Shore Islands (ESI) proposed Marine Protected Area (between 62° W and 63° W). The dashed line indicates the model domain and is bound by the 40-m isobath and longitudinal boundaries of the ESI.
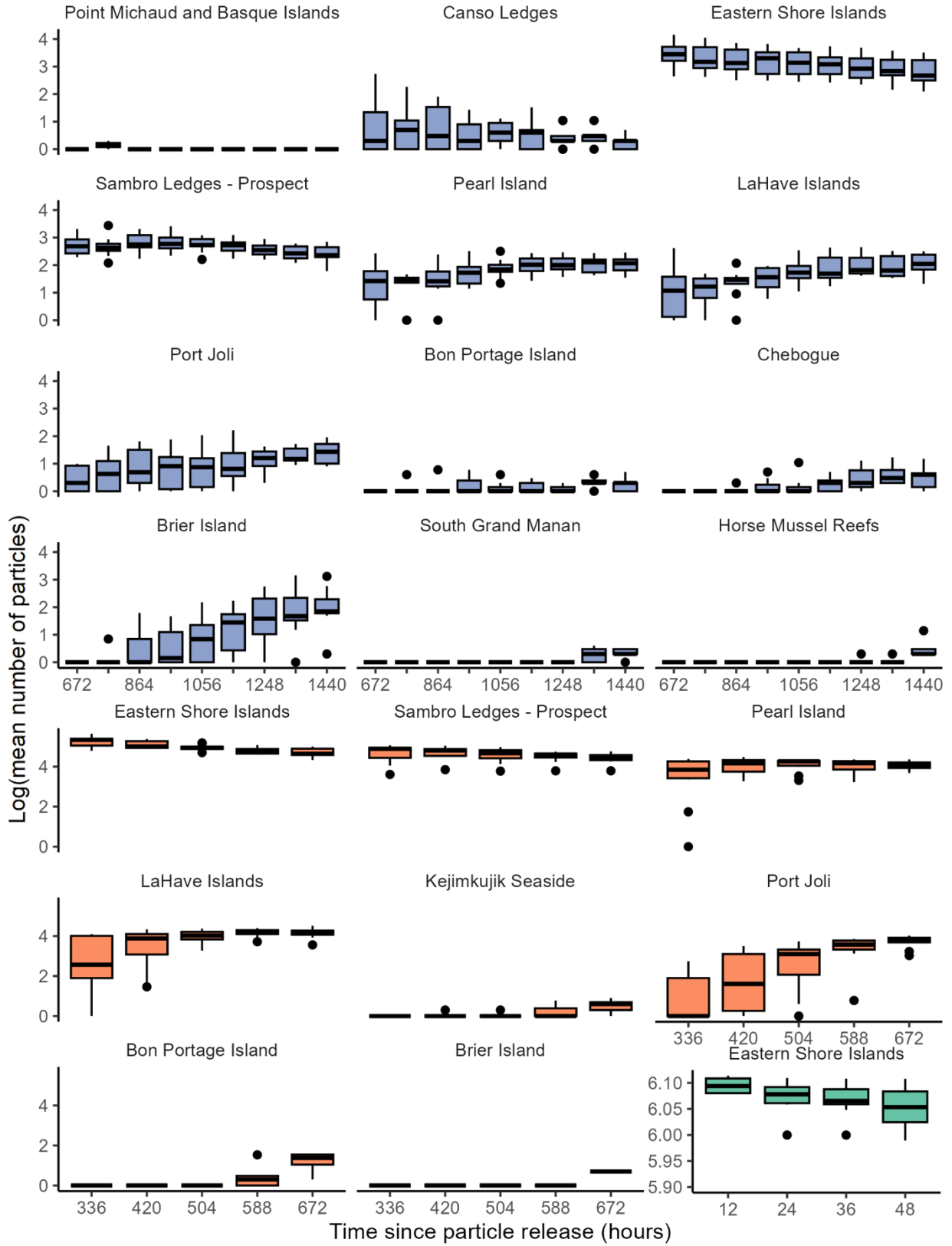
Figure S5: Log of mean number of particles (+ standard deviation) crossing the boundaries into each coastal proposed marine protected area (MPA) during the 3D simulations for laminarian kelps (green), *Membranipora membranacea* (orange), and *Strongylocentrotus droebachiensis* (purple) during their competent propagule duration (CPD). The label at the top of each plot indicates the name of the proposed coastal MPA. MPAs not reached by any particles during any simulation are not shown.

References

AWS pricing calculator. 2023. https://calculator.aws/#/addService?ch=cta&cta=lower-pricing-calc.

Greenlaw, M., A. Gromack, S. P. Basquill, D. Mackinnon, and R. Henry. 2013. A Physiographic Coastline Classification of the Scotian Shelf Bioregion and Environs: The Nova Scotia Coastline and the New Brunswick Fundy Shore. Page iv.

Supporting Information. Comparing approaches for estimating ecological connectivity at a local scale in a marine system.

SECTION 2: Supplementary methods

Details of random forest modelling

<u>Kelp habitat mapping</u>

In the drop camera surveys in 2017, 3-minute video clips (spanning 5 – 50 m in distance because of vessel drift) were collected at 10 cm – 2 m above the seafloor at a series of locations in a radial pattern from selected islands using a SV-HD-SVI camera (Shark Marine Technologies Inc., St. Catharines, Ontario; (Vandermeulen, 2017); $n = 445$) [for details see Vandermeulen (2018)]. In 2019, four 15 – 20 km-long video transects were sampled from inshore (~35 m depth) to offshore (~130 m depth), with the drop-camera Campod at ~1 m above the seafloor. From the Campod video, image framegrabs were extracted in ArcMap at 200-m intervals (Metaxas, Murillo-Perez, unpublished data; $n = 339$). Presence or absence of kelp habitat was recorded for each drop video or extracted image. We filtered the data to only include sample locations from within our model domain for training and validating the species distribution model (see below).

At 17 additional locations, we completed 100-120-meter transects with SCUBA using hand-held GoPro 2 or GoPro 5 cameras set to 1080 HD, at 6 and 9 m depth, between 4 and 9 August 2018. The camera was attached to a 1.5-m plumb line, allowing divers to swim at a constant height above the seafloor and providing a scale for post-processing images. We extracted frame-grabs from the video footage at 10-s intervals and evaluated every 3rd non-overlapping image (30-s interval) for percent cover of kelp habitat. We replaced images of poor quality by the preceding or ensuing one. Before analysis, we enhanced images by modifying the contrast, highlight and saturation settings using Photos for Windows. We extracted percent cover of kelp using the points method in ImageJ, where 100 points were overlaid on each image, and the feature directly behind each point recorded. In 2020, we conducted 17 150-m long transect surveys during which two snorkelers swam in parallel trajectories 2 m apart and recorded the presence/absence of kelp habitat.

<u>Species distribution modelling</u>

A digital elevation model and spatial layer of relative wave exposure at 35-m resolution were obtained from DFO (Greenlaw et al., 2013; O'Brien et al., 2022). A physiographic coastline classification map was based on Greenlaw et al. (2013). The coastline classification map was processed to create a binary variable for presence of hard substrate (1 = true, 0 = false) as suitable substrate for kelp (Appendix S1: Table S1). The relative wave exposure index is calculated as the product of fetch (f; in km), average wind speed (s; km h^{-1}), and wind frequency (k; percentage of time the wind blows in a particular direction), summed over 32 compass headings (Keddy, 1984):

$$Relative\ Wave\ Exposure\ Index = \sum_{i=1}^{32} f_i\ s_i\ k_i\ .(1)$$

Wind velocity data for the relative wave exposure index calculations were obtained from ERA5 through the Copernicus Climate Data Store at 0.25 ° resolution (Hersbach et al., 2018). All predictors were upscaled to a resolution of 210 m in raster format for the entire study domain. This spatial resolution represents an intermediate value between the spatial extent of observations at each point location (~ 50 m) and the distance between observation locations (~ 650 m).

We selected to use a random forest model because correlated predictor variables do not introduce bias. Additionally, a random forest model can be validated using "out-of-bag" data that is inherent in the model design due to bootstrap sampling. A random forest model is a type of classification and regression tree machine learning algorithm that 'grows' a forest of trees with bootstrap sampled data. Each tree is successively split into two groups based on a single random predictor (Breiman, 2001). The trees are then ensembled by majority vote. We divided our dataset into training and validation sets, using ⅔ and ⅓ of the full dataset, respectively. Model calculations were completed in R 4.0.2 using the *randomForest* package (Liaw and Wiener, 2002; R Core Team, 2020). We assessed the error of the final model using out of bag error, validation error, and the area under the precision-recall curve. Raw probabilities were converted to a binary "presence/absence" classification based on the precision-recall curve.

We defined kelp patches from the raw raster prediction by making assumptions about patch size and contiguity using the '*smoothr'* package in R (Strimas-Mackey, 2020). First, to remove noise introduced by the fine resolution raster grid, all cells classified as "absent", but contiguous to cells classified as "present" on all sides, were converted to "present". Next, we smoothed the edges of kelp patches, using Gaussian kernel regression. Since we aimed to release > 100,000 propagules per patch (see below), we only retained the largest kelp patches (threshold = 3 km^2) that encompassed the full spatial range across the ESI and resulted in a computationally feasible number of patches. The centroids of each of the resulting patches were used as the release point for propagules to calculate dispersal for kelps (*S. latissima* and *L. digitata*) and *M. membranacea*.

The current distribution of the sea urchin *S. droebachiensis* is limited because of mass mortality due to disease outbreaks caused by the amoeba *Paramoeba invadens* (Feehan and Scheibling, 2014). Based on a recent survey with the drop-camera Campod (see details in Kelp habitat mapping), the present depth range of *S. droebachiensis* in the ESI extends from 45 m to 100 m. We selected 16 locations in the survey transects (four per transect) of the drop-camera as release points for *S. droebachiensis* larvae along the depth range in which they were observed (45, 60, 75, and 90 m).

To determine the distribution of kelp in the ESI, we trained a random forest model that accounts for the main physical and geomorphic factors but were unable to represent the full

10

complexity of the ecosystem. Ocean properties including temperature, salinity and nitrate concentration were not included in the model due to a mismatch in resolution of available data. Biotic controls on kelp, such as distributions of the grazer *S. droebachiensis* and the invasive species *M. membranacea*, were also not included in the model. *S. droebachiensis* have experienced mass mortality events in recent years (Feehan and Scheibling, 2014) and are not currently present in kelp beds at ESI (personal observations). The invasive bryozoan *M. membranacea* can cause defoliation of kelp beds (Denley and Metaxas, 2017) but data resolution was not sufficient to include it as a predictor in the random forest model. However, we are confident that our random forest model provides a realistic distribution of kelp habitat in the ESI because of the accuracy of the validation set (79.3 %) combined with empirical validation of the model output in situ.

The random forest model produced a mosaic distribution of kelp patches in the Eastern Shore Islands (Appendix S1: Figure S2, Appendix S1: Figure S4). The depth range of predicted kelp patches was 0 – 41 m (mean: 17.75 m ± 8.74), and kelp beds were more often predicted in areas with a higher relative wave exposure. We optimized the random forest model with 500 trees and 2 variables randomly sampled for each split. The final model had an out of bag error of 20.7% and validation set error of 21.7% (Appendix S1: Table S5). Depth was the most important predictor variable, followed by relative wave exposure index and suitable habitat, with mean decreases in Gini index of 59.54, 53.43, and 31.14, respectively. The threshold from the precision-recall curve to convert estimated probabilities to presence/absence of kelp patches was 0.44 with associated recall and precision values of 0.729 and 0.723, respectively (Appendix S1: Figure S2). After post-processing of the distribution layer, there were 13 kelp patches occupying 329.4 km^2 or 31.6 % of the model domain area (depth < 40 m). The average patch size (after removing patches smaller than 3 km^2) was 25.3 km^2.

Calculation of rates of propagule release

Strongylocentrotus droebachiensis

We calculated the number of oocytes released per unit area following methods described in Meidel and Scheibling (2001). In the Eastern Shore Islands (ESI), urchins are found between 40 and 100 m at low densities (1.47 ± 1.55 ind m^{-2}). We measured test diameter of urchins and calculated adult density in 5-mm size classes from image framegrabs extracted from four 15 – 20 km-long video transects. These video transects, conducted in 2019, sampled from inshore (~35 m depth) to offshore (~130 m depth), with the drop-camera Campod at ~1 m above the seafloor (Metaxas, Murillo-Perez, unpublished data; n = 339). Based on these data, we used fecundity parameters for post-transitional barrens from Scheibling and Meidel (2001).

We calculated total wet body mass (B_j) for urchins in 5-mm size classes using a regression relationship developed by Meidel and Scheibling (2001).

$$B_j = e^{2.81\,lnj - 7.0} \ (1)$$

In equation 1, j is the median test diameter (mm) for each size class.

We calculated fecundity (E_j), in units of spawned dry mass (g), for urchins in 5-mm size classes. This relationship, developed by Meidel and Scheibling (2001), converts the proportion of wet to dry gonad weight spawned.

$$E_j = 0.249\,I_j R B_j \ (2)$$

In equation 2, I_i is the proportion of total body weight that is gonad, R is the proportion of gonad weight spawned, and B_j is total wet body weight (g), derived from equation 1.

We calculated the number of eggs spawned per unit area (O; oocytes m^{-2}), as the product of the number of eggs spawned for each adult female, summed across size classes.

$$O = \ Daf \ \textstyle\sum_j \left(p_j \frac{E_j}{5.56 \times 10^{-7}}\right) (3)$$

In equation 3, D is the average density of urchins (ind m^{-2}), a is the proportion of adults (test diameter greater than 25 mm), f is the proportion of females, p_j is the proportion of urchins in each size class, and 5.56 x 10^{-7} is the dry weight per egg (g).

For our calculations, we used values of I_j and R from Meidel and Scheibling (2001). We assumed a 1:1 sex ratio (f = 0.5) (Meidel and Scheibling 1998, 2001; (Filbee-Dexter and Scheibling, 2014; Meidel and Scheibling, 2001, 1998). We used empirical estimates of D, a, and p_j from the ESI. Lastly, we assumed a maximum fertilization rate of 18 %, based on calculations from a comparable density of urchins from (Wahle and Peckham, 1999) to convert number of eggs to zygotes.

Based on these calculations, sea urchins produce 4116 zygotes m^{-2}. We used the value of 5000 zygotes m^{-2} in the 3D model.

Membranipora membranacea

We calculated the number of oocytes released per unit area combined for the two dominant kelp substrates (*Saccharina latissima* and *Laminaria digitata*). We measured colonies of *M. membranacea* on each species of kelp in the ESI in 2019 (Attridge et al. in review, Pratt et al. 2021 and in review). Colonies were divided into five size classes (< 1 mm, 1 – 3 mm, 3 – 5 mm, 5 – 8 mm, and > 8 mm) following (Denley et al., 2019). We obtained average fecundity of *M. membranacea* colonies of each size class per kelp substrate from Denley et al. (2019).

$$O = \textstyle\sum_s \left(D_s \sum_j \left(C_{js} F_{js}\right)\right) (4)$$

In equation 4, O is the number of oocytes spawned per unit area (oocytes m^{-2}), s refers to each of the two numerically dominant kelp substrates (*S. latissima* and *L. digitata*), j refers to five size

12

classes, D_s is average density of kelp (ind m^{-2}), C_{js} is the number of *M. membranacea* colonies on each kelp plant, and F_{js} is the average number of oocytes released per colony.

Fertilization rates for oocytes are extremely high (at least 98 % fertilization success observed by (Temkin, 1994)) because fertilization occurs in the intertentacular organ after spermatozeugmata (an aggregate of 32 or 64 sperm) are drawn into the lophophore by feeding currents of *M. membranacea* colonies. We therefore assumed a fertilization rate of 100 %.

Based on these calculations, *M. membranacea* produce 135 055 zygotes m^{-2}. We used the value of 1 x 10^5 zygotes m^{-2} in the 3D model.

Laminarian kelps

We calculated the number of spores released per unit area (spores m^{-2}) for each of the two numerically dominant kelp species (*Laminaria digitata* and *Saccharina latissima*) using data from the field and literature.

$$P_s = a_s D_s A_s G_s H_s \times 2 \ (5)$$

In equation 5, P is the number of spores per unit area (spores m^{-2}), s represents each of the two dominant kelp species (*Saccharina latissima* and *Laminaria digitata*), a is the proportion of fecund plants, D is the average density of kelp (ind m^{-2}), A is the total sorus area per plant (cm^2), G is the average sporangial density (spores cm^{-2}), and H is the number of spores per sporangium. The calculated value of P$_s$ using equation (5) is multiplied by two to account for both sides of the kelp blade.

For our calculations, we used G values for each kelp species from (Chapman, 1984). We empirically measured the proportion of fecund plants (*a*) in the ESI in October 2021 using data from ten quadrats at each of three sites and each of two depths (6 m and 9 m) per site (Savard-Drouin & Metaxas, unpublished data). Data were pooled from all recorded kelps (n = 222 for *L. digitata* and n = 172 for *S. latissima*). We also collected reproductively mature kelps (10 per species for three sites at two time periods) to determine for sorus area (A_s) (Savard-Drouin, Metaxas unpublished data). We traced sorus area onto acetate sheets and then processed images in ImageJ (n = 59 for *L. digitata* and n = 59 for *S. latissima*). All empirical measurements were collected in October and November of 2021 and data were pooled across the two sampling periods. We assumed that each sporangium contained 32 spores, with a 1:1 sex ratio (Lüning, 1980; Schreiber, 1930). Therefore, we used a H_s value of 16. Based on our calculations, *L. digitata* and *S. latissima* will release 1.2 x 10^{10} and 1.1 x 10^{10} spores over one spawning season, respectively; however, only a small proportion differentiate into gametophytes (Gaylord et al., 2006). We divided the calculated number of released propagules by the ratio of spores to microscopic recruits measured by Chapman (1984), as 10^4 spores: 1 gametophyte. This approach allowed us to model an ecologically relevant number of propagules within our logistical capabilities.

Based on these calculations, kelps produce 1.2 x 10^6 spores of *Laminaria digitata* m^{-2} and 1.1 x 10^6 spores of *Saccharina latissima* m^{-2}. We used the value of 1 x 10^6 spores m^{-2} to represent spore production for both species combined in the 3D model.

References

AWS pricing calculator [WWW Document], 2023. . AWS. URL https://calculator.aws/#/addService?ch=cta&cta=lower-pricing-calc (accessed 5.4.23).

Breiman, L., 2001. Random Forests. Mach. Learn. 45, 5–32.

Chapman, A.R.O., 1984. Reproduction, recruitment and mortality in two species of Laminaria in southwest Nova Scotia. J. Exp. Mar. Bio. Ecol. 78, 99–109.

Denley, D., Metaxas, A., 2017. Lack of substrate specificity contributes to invasion success and persistence of *Membranipora membranacea* in the northwest Atlantic. Mar. Ecol. Prog. Ser. 580, 117–129.

Denley, D., Metaxas, A., Fennel, K., 2019. Community composition influences the population growth and ecological impact of invasive species in response to climate change. Oecologia 189, 537–548.

Feehan, C.J., Scheibling, R.E., 2014. Disease as a control of sea urchin populations in Nova Scotian kelp beds. Mar. Ecol. Prog. Ser. 500, 149–158.

Filbee-Dexter, K., Scheibling, R.E., 2014. Detrital kelp subsidy supports high reproductive condition of deep-living sea urchins in a sedimentary basin. Aquat. Biol. 23, 71–86.

Gaylord, B., Reed, D.C., Raimondi, P.T., Washburn, L., 2006. Macroalgal spore dispersal in coastal environments: Mechanistic insights revealed by theory and experiment. Ecol. Monogr. 76, 481–502.

Greenlaw, M., Gromack, A., Basquill, S.P., Mackinnon, D., Henry, R., 2013. A Physiographic Coastline Classification of the Scotian Shelf Bioregion and Environs: The Nova Scotia Coastline and the New Brunswick Fundy Shore, DFO Can. Sci. Advis. Sec. Res. Doc. 2012/051.

Hersbach, H., Bell, B., Berrisford, P., Biavati, G., Horányi, A., Muñoz Sabater J, Nicolas, J., Peubey, C., Radu, R., Rozum, I., Schepers, D., Simmons, A., Soci, C., Dee, D., J-N, T., 2018. ERA5 hourly data on pressure levels from 1979 to present. https://doi.org/10.24381/cds.bd0915c6

Keddy, P.A., 1984. Quantifying a within-lake gradient of wave energy in Gillfillan Lake, Nova Scotia. Can. J. Bot. 62, 301–309.

Liaw, A., Wiener, M., 2002. Classification and Regression by randomForest. R News.

Lüning, K., 1980. Critical levels of light and temperature regulating the gametogenesis of three Laminaria species (Phaeophyceae)1. J. Phycol. 16, 1–15.

Meidel, S.K., Scheibling, R.E., 2001. Variation in egg spawning among subpopulations of sea urchins *Strongylocentrotus droebachiensis*: a theoretical approach. Mar. Ecol. Prog. Ser. 213, 97–110.

Meidel, S.K., Scheibling, R.E., 1998. Annual reproductive cycle of the green sea urchin, *Strongylocentrotus droebachiensis*, in differing habitats in Nova Scotia, Canada. Mar. Biol. 131, 461–478.

O'Brien, J.M., Wong, M.C., Stanley, R.R.E., 2022. A relative wave exposure index for the coastal zone of the Scotian Shelf-Bay of Fundy Bioregion. https://doi.org/10.6084/m9.figshare.c.5433567

R Core Team, 2020. R: A Language and Environment for Statistical Computing.

Schreiber, E., 1930. Untersuchungen Über Parthenogenesis, Geschlechtsbestimmung und Bastardierungsvermögen bei Laminarien. Zeitschrift für wissenschaftliche Biologie. Abteilung E. Planta 12, 331–353.

Strimas-Mackey, M., 2020. smoothr: Smooth and Tidy Spatial Features.

Temkin, M.H., 1994. Gamete spawning and fertilization in the gymnolaemate bryozoan *Membranipora membranacea*. Biol. Bull. 187, 143–155.

Vandermeulen, H., 2017. A Drop Camera Survey of Port Joli, Nova Scotia (No. 3215). Can. Tech. Rep. Fish. Aquat. Sci.

Wahle, R.A., Peckham, S.H., 1999. Density-related reproductive trade-offs in the green sea urchin, *Strongylocentrotus droebachiensis*. Mar. Biol. 134, 127–137.